

Frascati Physics Series Vol. XXX (1997), pp. 000-000
HEAVY QUARKS AT FIXED TARGET - St. Goar, Oct 3rd, 1996

ANALYSIS OF SUBSTRUCTURES IN CHARM DECAYS

Sandra Malvezzi

*Istituto Nazionale di Fisica Nucleare-Sezione di Milano
Via Celoria 16, I-20133 Milan, Italy*

ABSTRACT

Recent results on Dalitz analysis of three-pseudoscalar decays are discussed in the context of probing charm hadronic-decay mechanisms: the role of FSI effects, which create phase shifts between the interfering resonant channels, can be studied in the different decay modes and the annihilation contribution measured in the charm sector through the $D_s^+ \rightarrow \pi^+\pi^-\pi^+$ decay.

1 Introduction

The analysis of substructures should be considered in the context of probing hadronic-decay dynamics. The quality of data and the availability of high-statistics samples have already shed a great deal of new experimental light on the non-leptonic decays of charm particles. Indeed, a full lifetime-hierarchy pattern has now been experimentally established ^{1, 2)}, posing severe constraints on theoretical models and pointing to hadronic-sector corrections. The importance of final-state interactions (FSI), in which the two decay daughters undergo strong rescattering after their initial formation, can be gauged from the isospin-amplitude interference. The factorization model predictions can be seriously distorted by FSI; the example of $D^0 \rightarrow K^+K^-/\pi^+\pi^-$ ratio, expected to be 1.4 (BSW ³⁾) and measured as ~ 2.5 ⁴⁾,

Table 1: *Isospin Decompositions.*

Mode	Ratio of amplitudes	$\delta = \delta_I - \delta_{I'}$
$K\pi$	$ A_{1/2} / A_{3/2} = 3.99 \pm 0.25$	$86^\circ \pm 8^\circ$
$K^*\pi$	$ A_{1/2} / A_{3/2} = 5.14 \pm 0.54$	$101^\circ \pm 14^\circ$
$K\rho$	$ A_{1/2} / A_{3/2} = 3.51 \pm 0.75$	$0^\circ \pm 40^\circ$
$K^*\rho$	$ A_{1/2} / A_{3/2} = 5.13 \pm 1.97$	$42^\circ \pm 48^\circ$
KK	$ A_1 / A_0 = 0.61 \pm 0.10$	$47^\circ \pm 10^\circ$
$\pi\pi$	$ A_2 / A_0 = 0.72 \pm 0.14$	$82^\circ \pm 9^\circ$

underscores their important role. In table 1 a list of phase shifts and isospin amplitudes ⁵⁾ is reported: the phase shifts between different isospin amplitudes are seen to be often approximately 90° , indicating the general importance of FSI.

Recently, amplitude analysis of non-leptonic decays has emerged as an excellent tool for studying charm hadron dynamics. In fact, deviations from flat Dalitz plots indicate non-constant dynamics and a knowledge of the quantum-mechanical decay amplitudes allows one to properly account for interference effects when calculating branching ratios. In addition, such an analysis provides new probes of FSI by measurement of the phase shifts between the interfering amplitudes for the various resonant channels. A problem, still unsolved in charm decay, is the reliable estimate of non-spectator contributions; $D_s^+ \rightarrow \pi^+\pi^-\pi^+$ is the best candidate to occur through an annihilation diagram since the annihilation of the two initial quarks is Cabibbo favoured and not suppressed as in the D^+ . Nevertheless, the presence of resonant channels with an $s\bar{s}$ quark content would suggest spectator processes rather than W annihilation, making a Dalitz-plot analysis necessary to disentangle direct three-body decays from resonances. Many experiments have focused on the substructure analysis; among the simplest decays to analyze are those of the ground-state charm mesons into three pseudoscalars:

$$\begin{aligned}
 D &\rightarrow K\pi\pi && (\text{Mark III }^6), \text{ E691 }^7), \text{ Argus }^8), \text{ E687 }^9)) \\
 D &\rightarrow KK\pi && (\text{E691 }^{10}), \text{ E687 }^{11})) \\
 D &\rightarrow \pi\pi\pi && (\text{E691 }^{12}), \text{ E687 [preliminary]}.
 \end{aligned}$$

2 $KK\pi$ Dalitz plots

The $D_s^+, D^+ \rightarrow K^+K^-\pi^+$ ¹ Dalitz plots in $m_{KK}^2, m_{K\pi}^2$, obtained by E687 and shown in fig. 1, are particularly instructive. The D_s^+ Dalitz is very highly dominated by

¹Through this paper the charge conjugate state is always implied.

the $\phi\pi^+$ and $\bar{K}^{*0}K^+$ channels while the D^+ has a significant additional contribution appearing as a uniform event intensity. Depopulation of the central region of the ϕ and \bar{K}^{*0} is due to a node in the decay function, reflecting angular-momentum conservation; the $\cos\theta_{\text{helicity}}$ (fig. 2) dependence is due to the vector nature of the mesons (ϕ, \bar{K}^{*0}) decaying into two pseudoscalars.

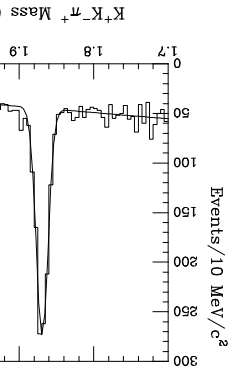


Figure 1: $KK\pi$ mass and Dalitz plots of the D^+ and D_s mass region.

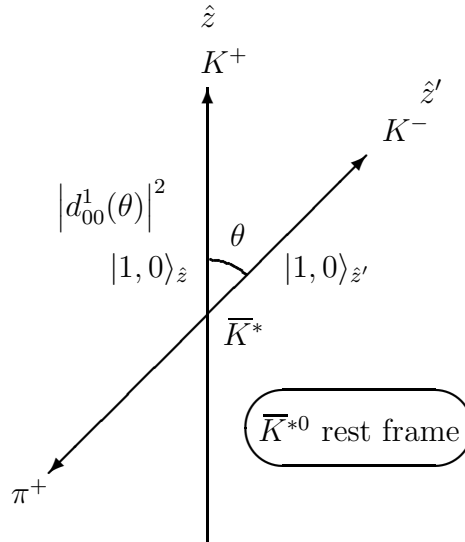


Figure 2: *Helicity angle definition.*

The Dalitz plots are fit with a coherent sum of resonances: quasi-two-body channels of the type

$$D \rightarrow \begin{array}{l} r + c \\ \quad \downarrow \\ \quad a + b, \end{array}$$

which are described by a decay function (eq. 1 and fig. 3),

$$\mathcal{M} = F_D F_r \times |\bar{c}|^J |\bar{a}|^J P_j(\cos \theta_{ac}^r) \times BW(m_{ab}). \quad (1)$$

The matrix element is the product of

- two vertex form factors (Blatt-Weisskopf momentum-dependent factors),
- an order J Legendre polynomial representing the decay angular wave function,
- a relativistic Breit-Wigner (BW).

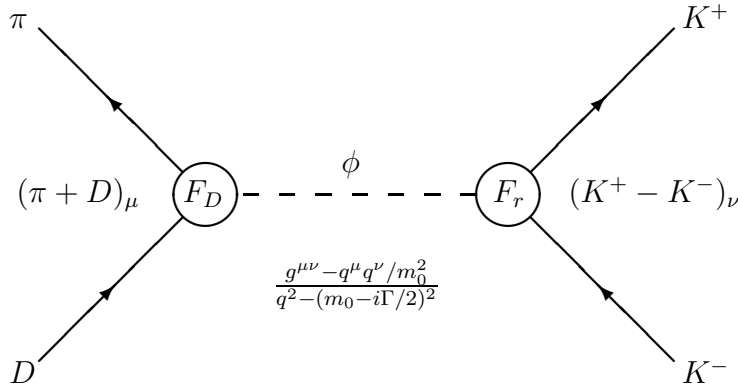


Figure 3: $D \rightarrow KK\pi$ decay diagram.

The total decay amplitude consists of various functions of the form (1), each multiplied by a complex factor $a_r e^{i\delta_r}$; in the simpler case of the D_s^+ , where only two contributions dominate ($\phi\pi^+$ and $\bar{K}^{*0}K^+$) the total amplitude is

$$\begin{aligned} \mathcal{A}(D_s^+ \rightarrow K^+ K^- \pi^+) &= a_{\bar{K}^{*0}} e^{i\delta_{\bar{K}^{*0}}} \mathcal{M}(\pi^+ K^- K^+ | \bar{K}^{*0}) \\ &+ a_\phi e^{i\delta_\phi} \mathcal{M}(K^+ K^- \pi^+ | \phi), \end{aligned} \quad (2)$$

where the modulus a measures the importance of the channel in the decay and δ is the phase. With the factorization hypothesis, the bare amplitudes will be real. Phases are then induced by FSI as consequence of Watson's theorem, which states that the observed amplitudes are related to the bare amplitudes by the square root of a strong-interaction S-matrix, describing the hadron-hadron scattering,

$$\begin{pmatrix} a_{\bar{K}^{*0}} e^{i\delta_{\bar{K}^{*0}}} \\ a_\phi e^{i\delta_\phi} \end{pmatrix}_{obs} = \begin{pmatrix} \eta e^{2i\delta_1} & i\sqrt{1-\eta^2} e^{i(\delta_1+\delta_2)} \\ i\sqrt{1-\eta^2} e^{i(\delta_1+\delta_2)} & \eta e^{2i\delta_2} \end{pmatrix}^{1/2} \begin{pmatrix} a_{\bar{K}^{*0}} \\ a_\phi \end{pmatrix}_{bare} \quad (3)$$

through the strong-interaction phase shifts ($\delta_{1,2}$) and the elasticity parameter (η). While FSI can be measured in two-body decays through the interference of isospin

amplitudes, in three-body decays they can be inferred from the interference of resonant channels, i.e., from the phase shifts. In practice, the phase of one resonance channel is factored out and hence relative phases are measured from experimental fits to $\mathcal{A}^*\mathcal{A}$. Visual evidence for FSI effects is possible through the study of the behaviour of the \bar{K}^{*0} lobes in $D^+ \rightarrow K^+K^-\pi^+$ (fig. 1). The asymmetry, not present in the D_s^+ case, can be interpreted as an interference effect (fig. 4) with a nearly constant amplitude (a broad scalar), which may be written as $\cos \delta + i \sin \delta$. The interference of these two amplitudes will produce a contribution to the intensity of the form

$$\begin{aligned}
& 2\text{Re}\left\{(\cos \delta + i \sin \delta)^* \frac{\cos \theta_{KK}}{m_r^2 - m_{K\pi}^2 - i\Gamma m_r}\right\} \\
&= 2 \frac{(m_r^2 - m_{K\pi}^2) \cos \theta_{KK} \cos \delta}{(m_r^2 - m_{K\pi}^2)^2 + \Gamma^2 m_r^2} + 2 \frac{\Gamma M_r \cos \theta_{KK} \sin \delta}{(m_r^2 - m_{K\pi}^2)^2 + \Gamma^2 m_r^2}. \quad (4)
\end{aligned}$$

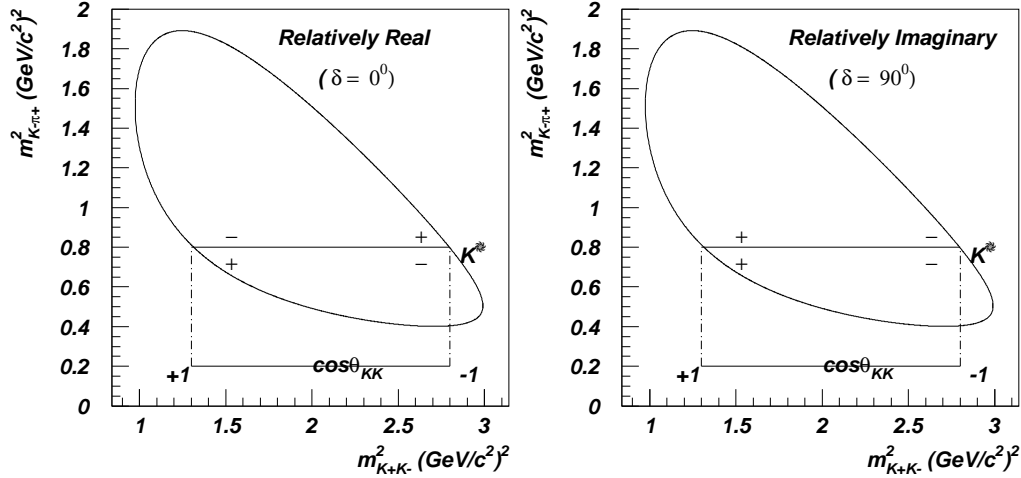


Figure 4: *The interference pattern of $D^+ \rightarrow KK\pi$ in the \bar{K}^{*0} band.*

As one moves along the \bar{K}^{*0} band in the direction of increasing m_{KK}^2 , $\cos \theta$ changes from $+1$ to -1 and both terms in eq. 4 switch sign. Along a line of constant m_{KK}^2 the first term, which dominates for a real amplitude ($\delta \sim 0^\circ$), switches sign on passing through the resonance pole (thus cancelling the interference), while the second interference term, which dominates for a relatively imaginary amplitude does not change sign under this motion. Thus, the patterns for real and imaginary phases are quite different; the interference present in the D^+ more closely resembles the pattern for a relatively imaginary amplitude, $\delta \sim 90^\circ$. A fully coherent Dalitz analysis of $D^+ \rightarrow K^+K^-\pi^+$ confirms this supposition (see table 2).

2.1 Speculation on the universality of Dalitz phases

Since the phase factors in the D^+ and D_s^+ both originate from FSI, one is tempted to speculate that they might be the same. In fact, if the D^+ and D_s^+ were degenerate in mass, the S -matrix describing the rescattering for $\phi\pi^+$ and $\bar{K}^{*0}K$ would be the same:

$$S = \begin{pmatrix} \eta e^{2i\delta_1} & i\sqrt{1-\eta^2}e^{i(\delta_1+\delta_2)} \\ i\sqrt{1-\eta^2}e^{i(\delta_1+\delta_2)} & \eta e^{2i\delta_2} \end{pmatrix}. \quad (5)$$

For elastic FSI ($\eta = 1$) it is easy to see that the observed amplitudes would then pick up a relative phase shift given by $\delta_1 - \delta_2$, which is common to D_s^+ and D^+ in the limit of degenerate masses. In this case, defining $R = (a_\phi/a_{\bar{K}^{*0}})_{phys.}$ and $R_0 = (a_\phi/a_{\bar{K}^{*0}})_{bare}$,

$$\begin{pmatrix} R \\ 1 \end{pmatrix} = \begin{pmatrix} e^{2i\alpha_\phi} & 0 \\ 0 & e^{2i\alpha_{K^*}} \end{pmatrix}^{1/2} \begin{pmatrix} R_0 \\ 1 \end{pmatrix} \quad (6)$$

and thus $\delta_\phi - \delta_{\bar{K}^{*0}} = \alpha_\phi - \alpha_{\bar{K}^{*0}}$ would be equal for both D^+ and D_s^+ . If $\eta < 1$, the observed phases would depend on the ratio of the ϕ and \bar{K}^{*0} amplitudes, which are different in the D_s^+ and D^+ and thus $\delta_\phi - \delta_{\bar{K}^{*0}}(D^+) \neq \delta_\phi - \delta_{\bar{K}^{*0}}(D_s^+)$. In the particular case of total inelasticity, $\eta = 0$,

$$\begin{pmatrix} R \\ 1 \end{pmatrix} = \begin{pmatrix} 0 & i \\ i & 0 \end{pmatrix}^{1/2} \begin{pmatrix} R_0 \\ 1 \end{pmatrix} = \frac{1}{\sqrt{2}} \begin{pmatrix} 1 & i \\ i & 1 \end{pmatrix} \begin{pmatrix} R_0 \\ 1 \end{pmatrix} \quad (7)$$

and $\delta_\phi - \delta_{K^*} = 90^\circ - 2 \tan^{-1} R_0$.

Thus, the universality of Dalitz amplitude phases might provide a clue to the elasticity of FSI. Table 2 compares the E687 final results for D^+ and D_s^+ ¹¹⁾ obtained through a fully coherent analysis, the total fit amplitude containing various K^+K^- and $K^-\pi^+$ resonances plus a flat non-resonant term. A few comments may be made on these results. The D^+ consists of nearly equal contributions of $\bar{K}(892)^{*0}K^+$, $\phi\pi$ and the broad scalar $\bar{K}(1430)^{*0}K$ while the D_s^+ is strongly dominated by just $\bar{K}^{*0}K^+$ and $\phi\pi^+$ plus a small contribution from $f_0(980)$ and $f_j(1710)$, which sum to 14%. Both the D^+ and D_s^+ can be fit by entirely quasi-two-body processes without the inclusion of a non-resonant contribution. It is interesting to note that both charm states have relatively real phases between the dominant $\bar{K}^{*0}K^+$ and $\phi\pi^+$ channels, $\sin(\delta_\phi - \delta_{\bar{K}^{*0}}) \approx 0$, which indicate absent or cancelling FSI phase shifts. In contrast, for the D^+ , $\sin(\delta_{\bar{K}(1430)^{*0}} - \delta_{\bar{K}(892)^{*0}}) \approx 0.94$, pointing to strong FSI effects, as anticipated in the discussion of the asymmetric \bar{K}^{*0} lobes, with the $\bar{K}(1430)^{*0}$ playing the role of the nearly constant scalar resonance. Unfortunately, the large error,

Table 2: Comparison of D^+ and $D_s^+ \rightarrow K^+K^-\pi^+$.²

Parameter	D^+	D_s^+
$\delta_{\bar{K}(892)^*0K}$	0° (fixed)	0° (fixed) \bar{K}^*
$\delta_{\phi\pi}$	$-159 \pm 8 \pm 11^\circ$	$178 \pm 20 \pm 24^\circ$
$\delta_{\bar{K}(1430)^*0K}$	$70 \pm 7 \pm 4^\circ$	$152 \pm 40 \pm 39^\circ$
$\delta_{f_0(980)\pi}$	-	$159 \pm 22 \pm 16^\circ$
$\delta_{f_j(1710)\pi}$	-	$110 \pm 20 \pm 17^\circ$
$f_{\bar{K}(892)^*0K}$	$0.301 \pm 0.020 \pm 0.025$	$0.478 \pm 0.046 \pm 0.040$
$f_{\phi\pi}$	$0.292 \pm 0.031 \pm 0.030$	$0.396 \pm 0.033 \pm 0.047$
$f_{\bar{K}(1430)^*0K}$	$0.370 \pm 0.035 \pm 0.018$	$0.093 \pm 0.032 \pm 0.032$
$f_{f_0(980)\pi}$	-	$0.110 \pm 0.035 \pm 0.026$
$f_{f_j(1710)\pi}$	-	$0.034 \pm 0.023 \pm 0.035$

$\sigma(\Delta\delta) = 56^\circ$, on the $\bar{K}(1430)^*0K$ relative phase for the D_s^+ precludes a meaningful test of the conjecture of a universal phase shift for this channel.

3 E687 preliminary results on $D_s^+, D^+ \rightarrow \pi^+\pi^-\pi^+$

The observation of a non-resonant three-pion decay of the D_s^+ would represent a clear signature in favour of non-spectator processes in the charm sector. To determine the rate of $D_s^+ \rightarrow \pi^+\pi^-\pi^+$ due to annihilation, the contributions from the resonant decays that most likely originate from the $s\bar{s}$ quark through spectator-diagrams have to be removed. The power of the E687 analysis is the *air-gap cut*, which imposes the requirement that the secondary vertex lies in the air-gap region downstream of the Be interaction target and upstream of any spectrometer elements. It significantly reduces the non-charm background and increases the signal-to-noise ratio by about a factor of four in both the D^+ and D_s^+ cases. In fig. 5 the invariant mass plots are shown with and without the air-gap cut. The large $K\pi\pi$ contamination, with the K misidentified as a π , is removed by requiring the candidate mass to be incompatible with the $D^+ \rightarrow K\pi\pi$ hypothesis. The Dalitz plots for the D^+ and D_s^+ signal regions, defined within $\pm 2\sigma$ from the mass peak, are shown in fig. 6. Owing to the presence of two identical particles, the $\pi^+\pi^-$ amplitudes have to be

²The fractions f_r are known as decay fractions and represent the ratio of the integrated Dalitz intensity for a single resonance r divided by the intensity with all contributions present

$$\text{decay fraction}_i = \frac{\int dm_{ab}^2 dm_{ac}^2 (a_i e^{i\delta_i} \mathcal{M}(abc|r))^* (a_i e^{i\delta_i} \mathcal{M}(abc|r))}{\int dm_{ab}^2 dm_{ac}^2 (\sum_i a_i e^{i\delta_i} \mathcal{M}(abc|r))^* (\sum_i a_i e^{i\delta_i} \mathcal{M}(abc|r))}.$$

Bose symmetrized; the representation chosen is that of a *folded* Dalitz plot where the lower and the higher value of the two possible $m_{\pi^+\pi^-}^2$ combinations are plotted on the abscissa and ordinate respectively.

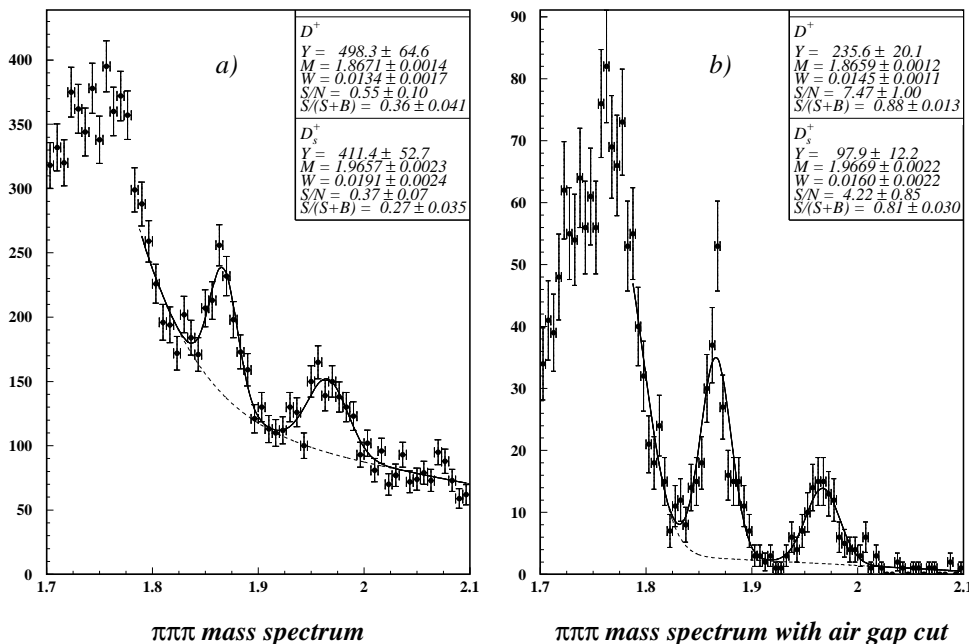


Figure 5: $\pi\pi$ mass spectrum a) without and b) with the air-gap cut.

Following the model already explained, the total amplitude is assumed to consist of a flat uniform term representing the non-resonant contribution plus a sum of functions representing the intermediate strong resonances and decay angular-momentum conservation. The fit parameters are then the amplitude coefficients a_i and phases δ_i . All the resonances decaying into $\pi^+\pi^-$ with sizeable branching fractions have been considered in the fit function. Fig. 7 shows the two mass projections of the Dalitz plots together with their sum. The resulting fit fractions and the relative phases are listed in table 3.

The D^+ appears to be largely dominated by the non-resonant and $\rho\pi^+$, with marginal contributions from the scalar $f_0(980)$ and the spin-2 resonance $f_2(1270)$. A signature for the $\rho(770)$ is the peak in the mass projections around $0.6 (\text{GeV}/c^2)^2$ and for the $f_0(980)$ the bump around $1.0 (\text{GeV}/c^2)^2$. The D_s^+ Dalitz plot, in contrast to the D^+ , is more structured. Even a visual inspection reveals the $f_0(980)$ band, previously observed by E691 ¹²⁾, and an accumulation of events at the sharp corner on the right side of the Dalitz plot, which could be attributed to the third helicity lobe of the $f_2(1270)$ plus an accumulation near the contour on the left side corresponding to

Table 3: D^+ and $D_s^+ \rightarrow \pi^+\pi^-\pi^+$ comparison.

Parameter	D^+	D_s^+
δ_{nr}	0° (fixed)	$235 \pm 22^\circ$
$\delta_{\rho\pi}$	$27 \pm 14^\circ$	$53 \pm 44^\circ$
$\delta_{f_2(1270)\pi}$	$207 \pm 17^\circ$	$100 \pm 18^\circ$
$\delta_{f_0(980)\pi}$	$197 \pm 28^\circ$	0° (fixed)
$\delta_{f_S(1500)\pi}$	-	$234 \pm 15^\circ$
f_{nr}	0.589 ± 0.105	0.121 ± 0.115
$f_{\rho\pi}$	0.289 ± 0.055	0.023 ± 0.027
$f_{f_2(1270)\pi}$	0.052 ± 0.034	0.123 ± 0.056
$f_{f_0(980)\pi}$	0.027 ± 0.031	1.074 ± 0.140
$f_{f_S(1500)\pi}$	-	0.274 ± 0.114

the first helicity-lobe region of the $f_2(1270)$. The non-resonant contribution appears to be marginal because of the absence of population in the upper corner of the Dalitz plot.

By way of contrast, a uniform-density horizontal band around $2.0 \text{ (GeV}/c^2)^2$ is manifest, whose structure suggests the presence of a scalar resonance in $\pi^+\pi^-$ mass around $1.5 \text{ (GeV}/c^2)$. Given the major uncertainty surrounding dipion scalar resonances in this mass region, the experiment decided to use its own data to find the parameters for a single state, which best reproduces the Dalitz plot. Several fits of D_s^+ Dalitz plot were performed by varying the mass (1200 MeV – 1600 MeV) and the width (25 MeV – 400 MeV) of this state, which was parametrized as a Breit-Wigner resonance. Fits were performed taking into account all possible additional contributions from a non-resonant component and the following well-established resonances, $f_0(980)$, $f_2(1270)$ and $\rho(770)$. A clear maximum of the likelihood function is found at $m = 1.475 \text{ GeV}/c^2$ and $\Gamma = 100 \text{ MeV}/c^2$. The parameters of this state, which is denoted as $\mathcal{S}(1500)$, are remarkably consistent with the $f_0(1500)$ entry of PDG96.³ Evidence for the non-resonant channel, as well as the $\rho\pi^+$ contribution, would have important implications for the theory; while the latter decay is expected to be heavily suppressed in the factorization model assuming isospin symmetry¹⁴⁾, the evidence of the non-resonant channel would indicate the presence of an initial-quark annihilation process. However, in contrast with the $\rho(770)\pi^+$ case, assessing the presence of the non-resonant component in a decay is a very difficult task, which

³Although the mass and width of this state are in excellent agreement with the $f_0(1500)$ entry in PDG96, it is to be emphasized that several interfering resonances could equally well describe the D_s^+ Dalitz plot.

would at least require a high-statistics sample since a coherent sum of wide resonances could easily mimic an almost flat contribution. A comparison of the D^+ and $D_s^+ \rightarrow \pi^+\pi^-\pi^+$ phase shifts (table 3) suggests a different and presumably more complex dynamics with respect to the $K^+K^-\pi^+$, with a different role of the FSI for D^+ and D_s^+ in this decay channel.

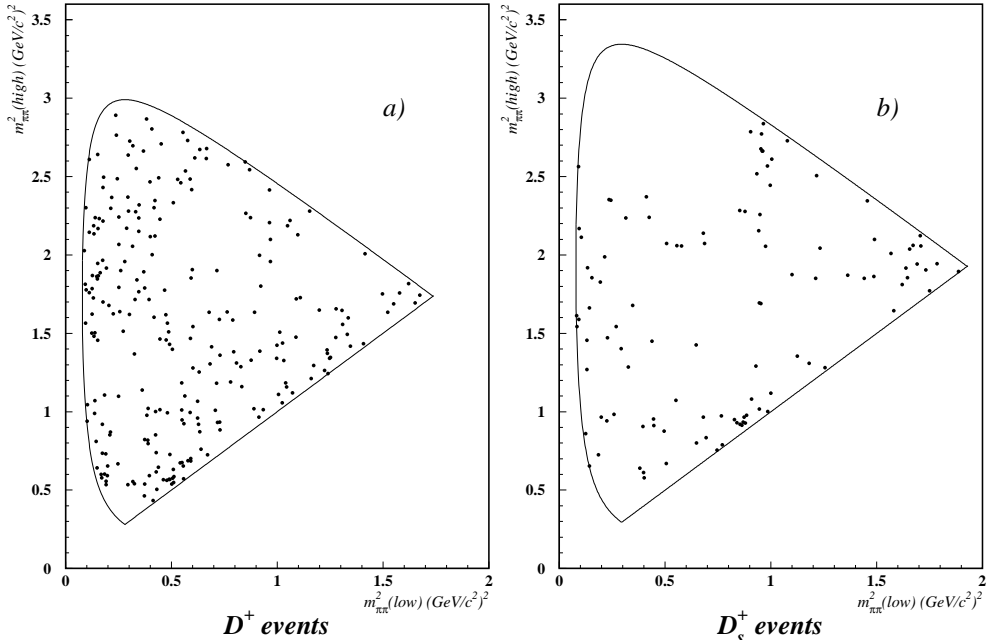


Figure 6: *Folded Dalitz plots for a) D^+ and b) $D_s^+ \rightarrow \pi\pi\pi$.*

4 $K\pi\pi$ Dalitz plots

The $K\pi\pi$ final state is the most studied so far: many experiments have focused on it and results are published for $D^+ \rightarrow K^-\pi^+\pi^+$, $D^0 \rightarrow K_s^0\pi^+\pi^-$ and $D^0 \rightarrow K^-\pi^+\pi^0$. A certainly striking conclusion reached by all groups is the presence of a large non-resonant component for $D^+ \rightarrow K^-\pi^+\pi^+$, which is unique to this decay, the majority of charm-meson decays being dominated by quasi-two-body processes. Furthermore, amplitude interference is significant in all three modes; the sum of the decay fractions, reported in table 4, greatly exceeds unity⁹⁾.

An analysis of the phase shifts is interesting also in this case: in table 5 the E687 $|\sin(\delta - \delta_{\bar{K}^*\pi})|$ is reported for the three modes.

It is interesting to note that the $\sin \Delta\delta$ values are consistent row by row: inelastic FSI or isospin phase shift could break this. One might also be tempted to affirm the

Table 4: *Sum of the $K\pi\pi$ final state decay fractions.*

	$K^-\pi^+\pi^+$	$K^0\pi^+\pi^-$	$K^-\pi^+\pi^0$
$\sum f_r$	1.47	1.27	1.18

Table 5: $|\sin(\delta - \delta_{\bar{K}^*\pi})|$ for the three $D^+ \rightarrow K\pi\pi$ modes.

	$K^-\pi^+\pi^+$	$K^0\pi^+\pi^-$	$K^-\pi^+\pi^0$
$\bar{K}\rho$	-	0.69 ± 0.1	0.31 ± 0.2
$\bar{K}^*(1430)\pi$	0.26 ± 0.09	0.24 ± 0.23	-
nr	0.74 ± 0.03	-	0.97 ± 0.25

presence of large FSI for $\bar{K}^*\pi$ relative to the non-resonant channel, but the issue here is to understand the precise nature of the non-resonant contribution: i.e., whether it is a single process or a mixture of broad resonances. In addition, although the amplitude model qualitatively reproduces many features of the data, statistically significant discrepancies are observed in some of the fits. This may be suggestive of strong-interaction dynamics not contained in the model, such as the presence of new, undiscovered wide resonances or a non-uniform, non-resonant amplitude with a possibly varying phase.

5 Conclusions

Dalitz-plot analysis has emerged as a powerful tool for studying hadronic charm decay, providing a new handle in dealing with FSI. In this context the recent high-statistics data have already furnished new interesting results: fully coherent analyses are now available for the $KK\pi$, $\pi\pi\pi$ and $K\pi\pi$ final states of the D mesons. These decays are found to be dominated by two-body resonances with the unique exception of $D^+ \rightarrow K^-\pi^+\pi^+$. Comprehension of the whole decay pattern depends on a correct parametrization of the non-resonant contribution, which could influence evaluation of amplitudes and phases. Attempts to improve the non-resonant flat dynamics, allowing a variation over the Dalitz plot, have been proposed¹³⁾ and will be implemented in the next analyses. Looking to the future prospects: exciting data are expected from the new E831 run (now in progress) while E791 should give results pretty soon. When the quality of the data allows a study of CP violation in the charm-meson sector through the measurement of the D and \bar{D} phases, a reliable estimate will require the ability to factor out the FSI induced phases.

6 Acknowledgements

I wish to acknowledge Prof. J.E. Wiss as being the first to address important issues in the Dalitz analysis and Drs. D. Menasce, L. Moroni, D. Pedrini and P.G. Ratcliffe for useful discussions.

References

1. P.L. Frabetti *et al.*, Phys. Lett. **B357**, 678 (1995).
2. S. Malvezzi, *Charm lifetime*: to appear in the Proc. Sixth International Symposium on Heavy Flavours Physics, Pisa, June 1995, e-print: hep-ph/9507391.
3. M. Bauer, B. Stech and M. Wirbel, Z. Phys. **C34**, 103 (1987).
4. PDG, R.M. Barnett *et al.*, Phys. Rev. **D54** (1996).
5. T. Browder, K. Honsheid and D. Pedrini, to appear in Ann. Rev. Nucl. Part. Sci. (1996).
6. J. Adler *et al.*, Phys. Lett. **B196**, 107 (1987).
7. J.C. Anjos *et al.*, Phys. Rev. **D48**, 56 (1993).
8. H. Albrecht *et al.*, Phys. Lett. **B308**, 435 (1993).
9. P.L. Frabetti *et al.*, Phys. Lett. **B331**, 217 (1994).
10. J.C. Anjos *et al.*, Phys. Rev. Lett. **60**, 897 (1988).
11. P.L. Frabetti *et al.*, Phys. Lett. **B351**, 591 (1995).
12. J.C. Anjos *et al.*, Phys. Rev. Lett. **62**, 125 (1989).
13. I. Bediaga, C. Gobél and R. Mendez-Galain, CBPF-NF-029 (May 1996), e-print: hep-ph/9605442.
14. M. Anselmino, I. Bediaga and E. Pedrazzi, CBPF-NF-045 (July 1995), e-print: hep-ph/9507292.

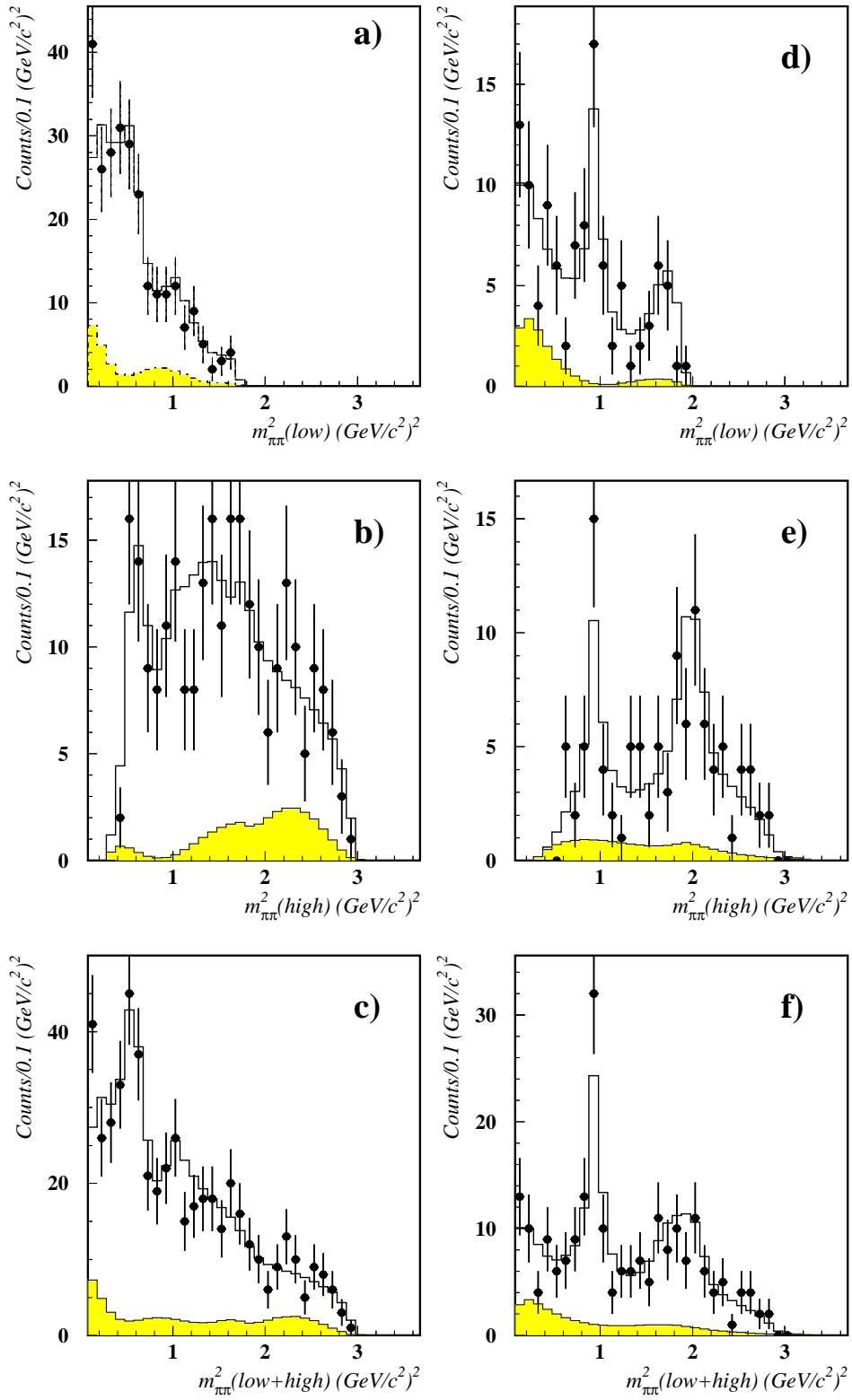


Figure 7: Invariant $\pi^+\pi^-$ mass projections for the D^+ : a) low, b) high, c) sum; and D_s^+ : d) low, e) high, f) sum. The crosses are data, the continuous line is the fit result and the shaded area represents the background.